Mito-TEMPO, A Selective Mitochondrial Antioxidant Alleviates Acrylamide-Mediated Anterior 2/3 Lingual Damage in Rats. Biochemical, Histological and Immunohistochemical Study

Heba Bayoumi[1], Enas Elgendy[1], Hala Taha Shalan[2], Ebtssam Beder[3], Nashwa Elsayed[4] and Amira Elalfy[1]

Original Article

[1]Department of Histology and Cell Biology, [4]Department of Medical Biochemistry and Molecular Biology, Faculty of Medicine, Benha University, Egypt

[2]Department of Anatomy and Embryology Department, Faculty of Medicine, Ain Shams University, Egypt

[3]Department of Forensic Medicine and Toxicology, Faculty of Veterinary Medicine, Benha university, Toukh, Egypt

ABSTRACT

Background: Acrylamide (ACR) is a common toxicant. One of the most critical worldwide health issues right now is the exposure of individuals and animals to ACR through their diet. Dietary antioxidants have received attention as potential preventive strategy and as a nutritional supplement for addressing various ACR-induced toxicities.

Aim of work: Studying the potential protective effect of Mito-TEMPO (MT) a selective mitochondrial antioxidant on acrylamide induced lingual toxicity.

Study design: Thirty two adult male rats were separated into 3 sets. Group I (control group). Group II (ACR group): Rats were treated with 40 mg/kg/d acrylamide that was dissolved in physiological saline and given orally by gavage for 14 days. Group III (ACR+ MT group): Rats were treated as group II and were injected with 0.7 mg/kg of Mito-TEMPO (ip) once/day for 2 days before acrylamide and continued with acrylamide for another 14 days. It was given 30 minutes before acrylamide.

Results: Acrylamide intoxicated group revealed significant decline ($P<0.001$) in the antioxidant enzymes levels, with marked degenerative changes in the dorsal, ventral and muscle core at the level of light and electron microscopic examination involved degenerated papillae, thin keratin layer, dorsal epithelial metaplasia, disfigured muscle core, congested blood vessels and atrophied ventral mucous membranes. Moreover, there was significant rise ($P<0.001$) in COX-2, IL1-β and P53 immunoexpression in examined lingual tissues. Mito-TEMPO pretreated group showed significant rise ($P<0.001$) in the antioxidant enzymes with apparent improvement in the histological structure involved restored papillae, nearly normal muscle core and mucous membranes, with significant decline ($P<0.001$) in COX-2, IL1-β and P53 immunoexpression.

Conclusion: Mito-TEMPO revealed potential protective effect on acrylamide induced lingual toxicity.

Received: 04 April 2023, **Accepted:** 08 May 2023

Key Words: Acrylamide, mito-TEMPO, lingual toxicity.

Corresponding Author: Heba Bayoumi, MD, Department of Histology and Cell Biology, Faculty of Medicine, Benha University, Egypt, **Tel.**: +20 10 9739 0300, **E-mail:** heba.bayoumi@fmed.bu.edu.eg

ISSN: 1110-0559, Vol. 47, No. 2

BACKGROUND

The tongue is an anatomical site that indicates the state of the body's health. In many cases, the mouth cavity becomes a crucial diagnostic location[1]. It is supposed that the lingual papillae act as an indicator of overall health, therefore any nutritional shortage or medicine poisoning would manifest to abnormalities to these papillae[2].

Acrylamide (ACR) is α, β-unsaturated molecule, water-soluble, odorless crystalline solid[3]. It is primarily used to create polyacrylamide, which is used in personal care products, as well as in a number of chemical industries, chemical grouting, and soil conditioning[4]. However after the startling discovery that acrylamide was contained in several commonly consumed foods, public health worries over acrylamide increased[5]. Every country showed variable levels of ACR in foods, which was consistent with their dietary habits and methods for preparing food. People are subjected to ACR directly by the high temperature preparation of food, such as frying, baking, and roasting. Moreover, food packing with polyacrylamide exposes consumers indirectly to leftover ACR monomer[6].

 DOI: 10.21608/ejh.2023.203954.1879

Additionally, concerns have been expressed that children may be at an increased danger for acrylamide exposure owing to their increased nutritional consumption[7].

Its monomeric state is very carcinogenic, teratogenic, and neurotoxic to rats and mice while its polymeric state is non-toxic[8]. Acrylamide is strongly related to the development of cancer in humans, particularly in the oral cavity, colon, prostate, rectum, esophagus, large intestine and larynx[9].

ACR is characterized by high water solubility and small molecular weight, so, it is able to permeate through cell membranes fast, quickly absorbed and widely distributed throughout the body after oral intake[10]. It is effortlessly absorbed by the digestive system. It has been discovered to cause harm to the gastrointestinal mucosa by increasing inflammatory responses, oxidative stress, and cell death[11]. From this angle, research is increasingly concentrating on finding ways to reduce toxicity in *vivo* by minimizing oxidative harm caused by the ACR.

Antioxidants were used to reduce the formation of waste metabolic products and enhance the removal of reactive oxygen species (ROS)[12]. While natural antioxidant cannot reduce oxidative stress, antioxidant supplements may improve the organism's ability to do so[13]. Owing to the fact that mitochondrial malfunction contributes to a number of common diseases, the use of mitochondria-targeted antioxidants as a therapy is becoming more widespread[14].

We are not aware of any studies that used the selective mitochondrial antioxidant Mito-TEMPO (MT) to counteract the cytotoxic effects of ACR on the rat tongue mucosa and underlying muscle. Thus, the goal of this research is to analyze the histological, immunohistochemical, and ultrastructural effects of ACR on the rat tongue in order to provide guidance to examine the potential protective impact of Mito-TEMPO co-administration.

MATERIAL AND METHODS

Chemicals

Acrylamide (99.9 purity) at a form of white, odorless crystals at room temperature. Its molecular formula is C3H5NO.

Mito-TEMPO (Mito-T): at a form of white powder. Empirical Formula: C29H35N2O2P · Cl.

Both drugs were got from Sigma-Aldrich Company, St. Louis, MO, USA)

Animals and Ethical approval

Ethics committee approval (No: BUFVTM 07-12-22) of the animal care and experimental protocols and procedures were revised and accepted for the study by ethical committee in the Faculty of veterinary Medicine, Moshtohor, Benha University.

The 32 adult, healthy male albino-type rats used in the current study ranged in weight from 180 to 220g. The animals were housed in controlled environments with a 12-hour light-dark cycle, controlled room temperature, and controlled humidity levels (30–35%). They were fed with regular pellet rat food, which gave them full access to water.

Experimental design (Figure 1)

The model size of the current research was divided into 3 sets after a week of adaptation.

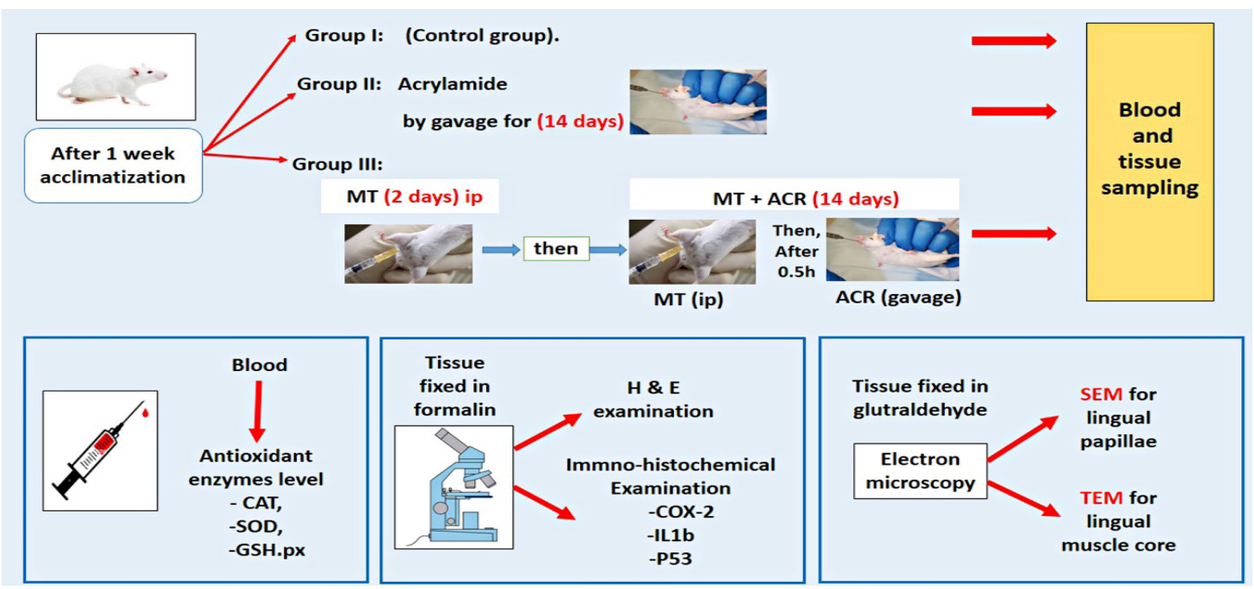

Fig. 1: Diagrammatic illustration summarizing the study design

Group I (Control group; 12 rats): Three subgroups of rats were similarly divided (each subgroup =4 rats).

- Ia: Rats were not given any drugs.
- Ib: Rats were treated orally by gavage with 0.5 ml/ rat of physiological saline for 14 days (vehicle for Acrylamide).
- Ic: Rats were injected with physiological saline intraperitoneally once daily for 2 days before beginning of oral saline and continued with oral saline for another 14 days.

Group II (ACR group; 10 rats): Rats were treated with 40 mg/kg/d acrylamide that was dissolved in saline and orally administered (0.5 ml/ rat) by gavage for 14 days[15].

Group III (ACR+ MT group; 10 rats): Rats in this group treated as group II and were injected with 0.7 mg/ kg of Mito-TEMPO dissolved in saline intraperitoneally[16] once daily for 2 days before beginning acrylamide and continued with acrylamide for another 14 days (Mito-TEMPO was given 0.5 hour before acrylamide).

Serological investigations

The following day after last ACR and Mito-TEMPO doses, ether was used to anesthetize rats. Blood samples (5ml) were taken from their hearts in heparinized tubes, centrifuged at (1500 × g for ten minutes) to obtain the serum, and stored at (−85°C) to analyze antioxidant parameters: catalase (CAT)[17], superoxide dismutase (SOD)[18] and glutathione peroxidase (GSH.Px)[19], using commercial kits (Rel Assay Diagnostics, Gaziantep, Turkey). The samples were measured at the Central Research Lab, Faculty of veterinary Medicine, Moshtohor, Benha University.

Histological study

Half of the tongue samples were preserved in 10% neutral formaldehyde to prepare wax blocks. Paraffin sections of (5-7 µm) thickness were cut by leica ordinary microtome from the paraffin blocks, stained with Hematoxylin and Eosin (H&E) according to[20], and examined under a light microscope to study the histopathological variations in the study groups.

Immunohistochemical (IHC) Study

Additional sections were fixed on +ve charged slides for IHC staining:

1. Immuno-staining for cyclooxygenase-2 (COX-2) antibody (oxidative stress marker); using rabbit polyclonal antibody (Lab Vision, cat N: PA1-37505). Cox-II positive reaction is detected as brown cytoplasmic color.
2. Immuno-staining for IL1-β antibody (inflammatory marker); using a commercial kit (anti-IL-1β dilution (1/200) Cell Signaling Technology, Danvers, MA). IL-1β positive reaction is detected as brown cytoplasmic color.
3. Immuno-staining for P53 antibody (cell death marker); using rabbit polyclonal antibody (cat. N: ab1431, 1/100; Abcam, Cambridg, UK). P53 positive reaction is detected as brown nuclear reaction.

The immunostaining was done using the avidin-biotin complex technique[21]. Simply; the activity of endogenous peroxidase was inhibited by rehydrating deparaffinized sections and incubating them for 30 minutes with 0.01% H_2O_2 solution. To hide the antigenic location, the tissues were then incubated for an additional 10 minutes in ethanol before being placed in a 0.01-M citrate buffer at pH=6. After twenty minutes in the microwave, the antigen was removed. The 1ry antibodies were applied to sections all-night at 4 °C using diluted versions for each protein. The avidin-biotin complex (ABC) reagent was then reacted with the sections for 1h, followed by 6–10 minutes of peroxidase solution. Following that, hematoxylin was used as a counterstain. Negative control slides were prepared by using PBS instead of primary antibodies.

Electron microscopic study

The remaining tongue samples were preserved in glutaraldehyde and used for EM examination.

a- Transmission electron microscopy (TEM)[22].

The muscle core of the anterior 2/3 of tongue samples were cut into small parts (about one mm3) for electron microscopic examination, prefixed in 2.5% glutaraldehyde for 120 minutes, then post-fixed in 1% osmium tetra-oxide for 120 minutes. Then, specimens were dehydrated and inserted in epoxy resin to get resin blocks. A Leica ultracut (UCT) was used to cut semithin and ultrathin sections (Glienicker, Berlin, Germany). Toluidine blue was used to stain the semithin (0.5 µm thick) slices (1%) and viewed under a light microscope. A two-step staining procedure using uranyl acetate 5% for 15 minutes and lead citrate for eight minutes was used to color ultrathin sections, which were cut at a thickness of 80-90 nm, put on copper grids, and stained. Sections were inspected and electron microphotographs were taken by a transmission electron microscope (JEOL TEM; 100 CX; Japan) at the Faculty of Science, El-Shatby, Alexandria University, Alexandria, Egypt.

b- Scanning electron microscopy (SEM)[23]:

Axial tongue tissues were cut to preserve only the dorsum and were fixed in 4% glutaraldehyde, then post fixed in 1% osmium tetroxide, dehydrated in up-graded ethanol concentrations, placed into amyl acetate, dried with critical-point dryer (E-3000) and covered by gold particles by a sputter coater (SPI-Module). The specimens were stored over silica gel. The dorsum of the tongue samples was scanned under SEM (JEOL: JSM-636- OLA, accelerating voltage: 15kv) at the Faculty of Science, El-Shatby, Alexandria University, Alexandria, Egypt.

Morphometric study

Two slides from each rats of each group were

assessed. Two random fields/slide from each animal were appraised. The mean area percentage (area %) of positive immunoreaction of COX-2, IL1-β and P53 were assessed in the non-overlapping fields of each section at (X200) magnification. The immune-sections were photographed by camera (Olympus; model: E24-10 M pixel, China) fixed on an Olympus microscope with a × 0.5 photo adaptor. The resulting photomicrographs were analyzed at central research lab, Moshtohor faculty of veterinary medicine, Benha University.

Statistical results evaluation

All data were statistically estimated by statistical Package for Social Science software program version N: 23 (IBM SPSS, Inc., USA). One-way analysis of variance (ANOVA) followed by "Tuckey" post-hoc test was used to conclude the statistical significance between different groups (*p value* <0.001 was considered to specify statistical significance). Statistics were presented as mean ±standard deviation (SD).

RESULTS

Histo-pathological studies

The normal tongue panoramic morphology showed the different parts of the ant 2/3 of rat tongue. The dorsal surface, muscle core and the ventral surface. (Figure 2)

Mito-TEMPO protected the tongue structure from the toxic effect of acrylamide:

On exposure to acrylamide for (14 days), noticeable degenerative changes that involved the dorsal, muscle core as well as the ventral surface were observed compared to control group. These degenerative changes were improved in co-treatment with MT.

The dorsal surface

Two forms of papillae were studied in the dorsal surface (Filiform papillae and fungiform papillae).

Filiform papillae

In H&E results the dorsum of control group showed many regular filiform papillae with tips directed backwards. The different cells showed vesicular nuclei (Figure 3a). In ACR-group (II), degenerated filiform papillae with broken tips and disfigured detached keratin layer. Some areas of the epithelial covering displayed focal metaplasia. Dilated blood vessel of the lamina propria with shallow epithelial ridges were apparent (Figure 3b). Co-treatment with MT showed nearly normal dorsal surface with few vacuolated cells (Figure 3c).

Fungiform papillae

Control group also showed normal appearance of fungiform papilla with characteristic mushroom-shape containing taste bud (Figure 4a). In ACR group we noticed thin atrophied fungiform papillae with absent taste bud. The adjacent filiform papillae showed lost tips and disfigured keratin covering (Figure 4b). Co-treatment with MT improved the fungiform papillae morphology with apparent taste bud (Figure 4c).

Muscle core

In control group; the muscular core was formed of striated muscle fibers oriented in longitudinal and tranvrse directions with peripheral vesicular nuclei (Figure 5a). On exposure to acrylamide for 14 days, the muscle core revealed highly degenerative changes with obvious fibers fragmentation. Some fibers were pale acidophilic, others were deep acidophilic with pyknotic nuclei. Huge congested blood vessels were remarkable (Figure 5b). In MT pre-treated group; the muscle showed nearly normal muscle fibers that were oriented in different directions with fatty infiltration in the connective tissuein-between the fibers (Figure 5c).

Ventral surface

The ventral mucous membrane of control group was smooth formed of stratified squamous keratinized epithelium with underlying lamina propria (Figure 6a). The ventrum showed apparent thinning with thin, detached keratin layer. The Lamina propria revealed congested blood vessels (Figure 6b). In MT pretreated group, the ventral surface showed improved histological appearance except for some vacuolated cells (Figure 6c)

Mito-TEMPO protected the tongue tissue via antioxidant, anti-inflammatory and anti-apoptotic effects

COX-2 immuno-expression

Examination of COX-2 immunostained sections of tongue of control groups exhibited negative staining reactivity of cells of the dorsal, muscle core and ventral surface (Figures 7 a,d,g). In contrast, lingual tissues of rats treated with ACR for short period (14 days) demonstrated A robust positive staining reactivity especially in the lamina propria of the dorsal and ventral surfaces (Figures 7 b,h) in addition to in the muscular core (Figure 7e). Lingual mucosa of dorsal and ventral surfaces of rats pretreated with MT as protective drug displayed mild positive staining reactivity in lamina propria (Figures 7 c,i.) along with the muscle core (Figure 7f)

IL1-β immuno-expression results

Regarding the results of lingual sections immunostained with IL1-β antibody, lingual sections of control groups exhibited minimal staining reactivity in the dorsal surface and muscle core as well as the ventral surface (Figures 8 a,d,g). Moreover, exposure to ACR, lingual sections demonstrated strongly positive staining reactivity in the epithelial lining, lamina propria of the both dorsal and ventral surfaces (Figures 8 b,h) as well as in most areas of the muscular core (Figure 8e). Lingual tissues of rats pretreated with MT as protective drug displayed mild positive staining reactivity in the underlying lamina propria of dorsal and ventral surfaces (Figures 8 c,i.) as well as in the muscle core (Figure 8f)

P53 immuno-expression results

Regarding the results of lingual mucosa immunostained with P53 antibody, lingual sections of control groups exhibited minimal staining reactivity in the dorsal surface, muscle core and ventral surface (Figures 9 a,d,g). Moreover, exposure to ACR caused strongly positive staining reactivity in the epithelial lining, lamina propria of the both dorsal and ventral surfaces (Figures 9 b,h) as well as in most areas of the muscular core (Figure 9e). Lingual tissues of rats pretreated with MT displayed decreased staining reactivity in the cells of dorsal and ventral mucous membrane and the underlying lamina propria (Figures 9 c,i.) as well as in the muscle core (Figure 9f).

Mito-TEMPO protected the tongue ultrastructure from the toxic effect of acrylamide:

SEM

The scanning panoramic morphology of control group tongue showed numerous conical filiform papillae with tapering ends directed caudally. Few fungiform papillae with wide apices are scattered in-between the filiform ones (Figure 10).

Filiform papillae

Two types of filiform papillae were studied in the dorsal surface (simple conic filiform papillae and giant filiform papillae with two tips).

Simple conic filiform papillae

SEM results showed in control group normal filiform papillae with normal length and tips directed backward (Figure 11a). In group II, the papillae were atrophied with narrow tips (Figure 11b), while in MT pretreated group they appeared nearly normal (Figure 11c).

Giant filiform papillae with two tips

SEM results showed in control group multiple normal giant filiform papillae with smooth double tips (Figure 12a). ACR group revealed abnormal giant filiform papillae with broken ends and outer desquamation (Figure 12b). While, in MT pretreated group the giant filiform papillae mostly appeared nearly normal with smooth tips (Figure 12c). .

Fungiform papillae

In control group, fungiform papillae appeared as normal mushroom like fungiform with taste pores (Figure 13a), surrounded by filiform papillae. In group II, the papillae were atrophied with unnoticeable taste pores (Figure 13b), while in MT pretreated group they showed remarkable ultrastructural improvement (Figure 13c).

TEM

The myofibrils oriented parallel to the long axis of the muscle and separated by rows of mitochondria. The sarcomeres had alternating dark A band and light I bands with evident electron-dense Z lines (Figure 14a). But in group II the muscle fibers displayed dark nuclei with heterochromatin. Disorganized muscular striation with areas of narrowing of the myofibrils and Z line irregularities were also evident. Moreover, clumps of rounded swollen mitochondria with dilated cristae appeared. (Figure 14b). MT pretreated group examination; reveled nearly normal orientation of muscle fibers with rows of mitochondria in-between (Figure 14c).

Morphometric studies

The antioxidant defense system, which includes the enzymes CAT, SOD, and GSH-Px, aids in the control of oxido-reductive homeostasis and the prevention of oxidative assaults on cells. The significant decline of CAT, SOD and GSH-Px levels ($p<0.001$) observed in the intoxicated rats when compared with normal control might be responsible for the toxicity of ACR. In MT pretreated group, these enzymes showed significant raised levels ($p<0.001$) when compared to control group (Table. 1) and (Figure 15a). As regarding the immune results, group II showed significant rise ($p<0.001$) in COX-2, IL-1β and P53 immunostaining, while group III showed significant decline ($p<0.001$) in COX-2, IL-1β and P53 immunostaining (Table. 2) and (Figures 15 b,c,d).

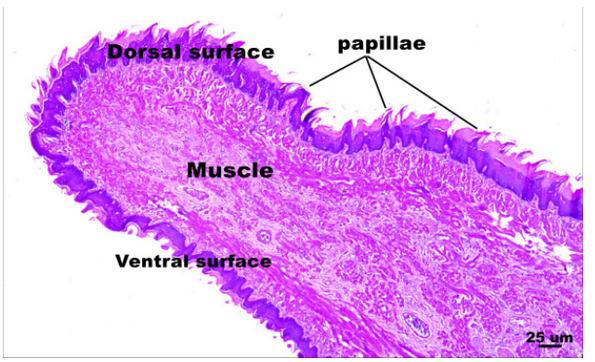

Fig. 2: A photomicrograph of longitudinal section in the ant 2/3 of rat tongue of the control group showing: Three parts of the ant 2/3 of the tongue. Rough mucous membrane covering the dorsum, formed of keratinized stratified squamous epithelium displaying lingual papillae. The muscle core is composed of interlacing striated muscle bundles running in different directions. Smooth mucous membrane covering the ventrum and lacking papillae. (H & E, Orig. mag. X40, scale bar = 25 µm)

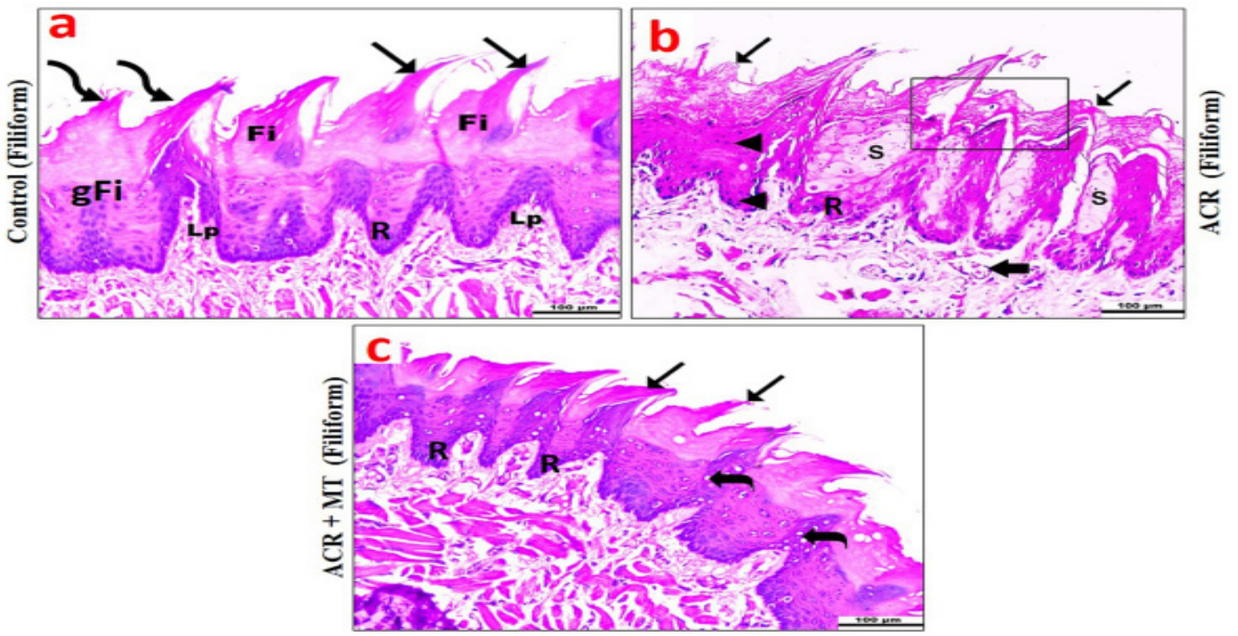

Fig. 3: A set of photomicrographs of longitudinal sections in the dorsal ant 2/3 of tongues from study groups showing filiform papillae: (a) Control group: regular dispersion of two types of filiform papillae; the simple conic filiform papillae (Fi) with slender pended tips (arrows), and the giant papillae (gFi) with two tips (bent arrows) with underlying layer of lamina propria (Lp). The papillae are showing normal epithelial ridges (R). (b) ACR group: filiform papillae showing foci of sebaceous gland-like metaplasia (S), pyknotic nuclei in some other cells (triangles), broken papillary tips (arrows) and disfigured keratin layer (rectangle). Notice; dilated blood vessel of the lamina propria (blunt arrow). (c) ACR+ MT group: nearly normal filiform papillae with normal tips (arrows) and epithelial ridges (R). Some cells showing slightly vacuolated cytoplasm (bent arrows). (H & E, Orig. mag. X200, scale bar = 100 µm).

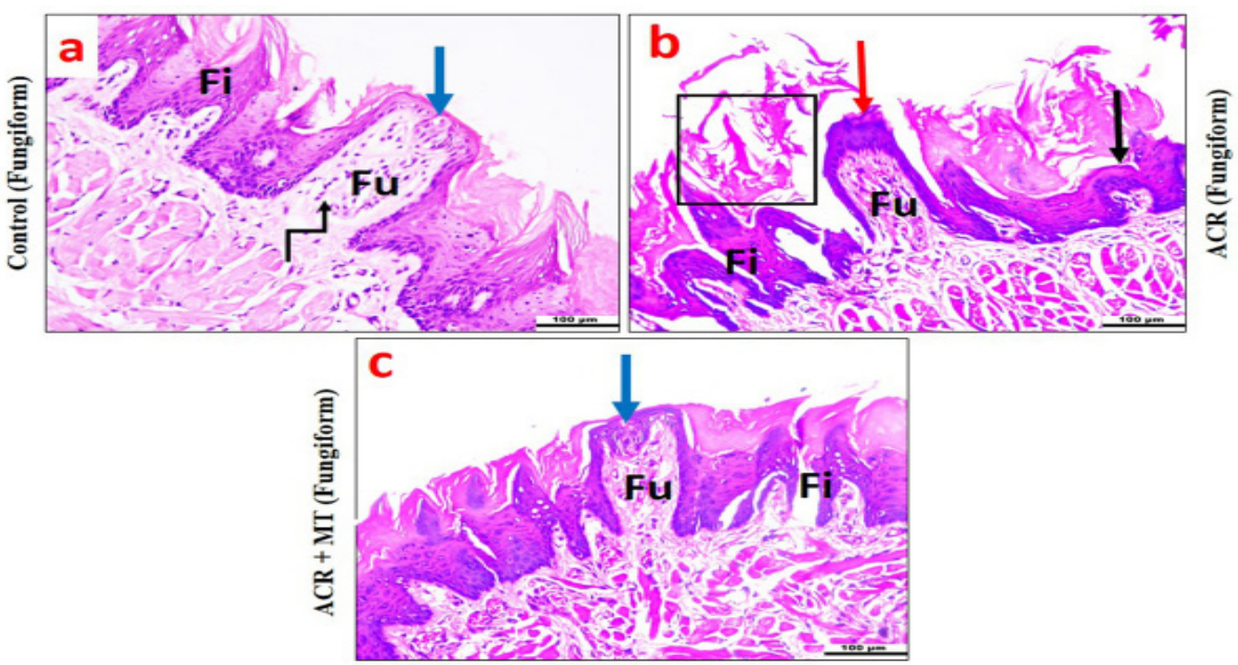

Fig. 4: A set of photomicrographs of longitudinal sections in the dorsal ant 2/3 of tongues from study groups showing fugiform papillae:
(a) Control group: Normal appearance of fungiform papilla (Fu) between filiform ones (Fi). Fungiform papilla appears as mushroom-shaped containing taste bud in the upper wide surface (blue arrow) and a core of connective tissue (angled arrow). (b) ACR group: Thin atrophied fungiform papilla (Fu) with absent taste bud. The tip of the papilla showing hypercellularity (red arrow). Some adjacent filiform papillae (Fi) showing lost tips (black arrow) and disfigured keratin covering (rectangle). (c) ACR+ MT group: Fungiform papillae appear nearly normal with taste bud (blue arrow). (H & E, Orig. mag. X200, scale bar = 100 µm).

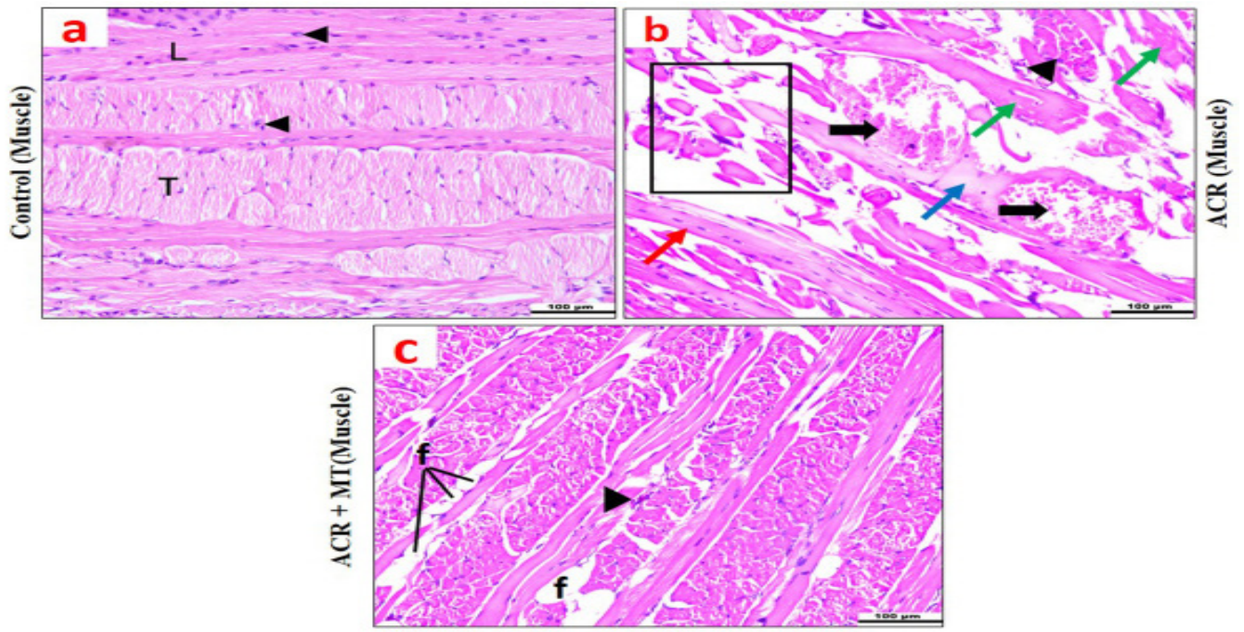

Fig. 5: A set of photomicrographs of longitudinal sections in the muscle core of the ant 2/3 of tongues from study groups showing: (a) Control group: normal arrangement of skeletal muscle fibers. The fibers are multinucleated with peripheral, oval vesicular nuclei (triangles). Some fibers are transverse (T), other fibers are longitudinal (L). (b) ACR group: loss of the normal histological morphology. Most fibers are fragmented (rectangle) with pyknotic nuclei (triangle), some fibers are pale acidophilic (blue arrow), but others are deeply acidophilic (green arrows). Some fibers appear with central nuclei (red arrow). Notice; multiple huge congested blood vessels (blunt arrows). (c) ACR+ MT group: most of the muscle fibers appear histologically improved. Fatty infiltration (f) in the connective tissue, and some pyknotic nuclei (triangle) can be seen. (H & E, Orig. mag. X200, scale bar = 100 µm).

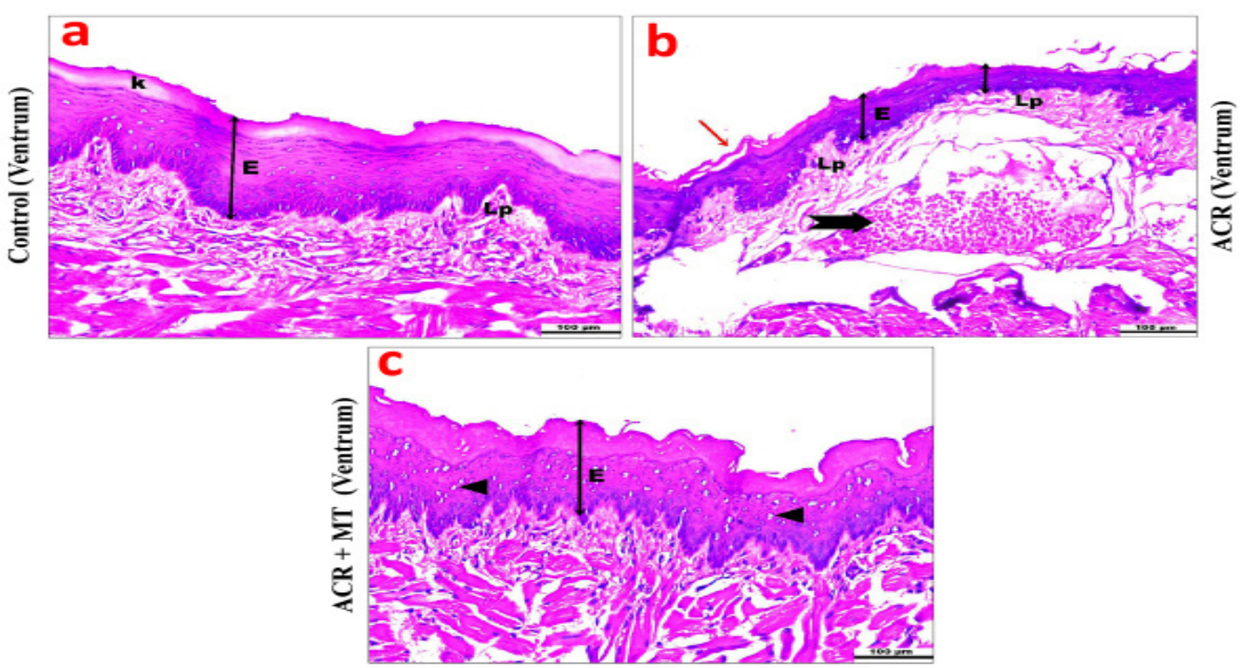

Fig. 6: A set of photomicrographs of longitudinal sections in the ventral surface of the ant 2/3 of tongues from study groups showing: (a) Control group: Smooth mucous membrane composed of stratified squamous epithelium (E) with keratin cover (k) and underlying lamina propria (Lp). (b) ACR group: The ventral mucous membrane is apparently thin with thin keratin layer showing focal detachment (red arrow). Huge congested blood vessel can be seen in the lamina propria (bifid arrow). (c) ACR+ MT group: the mucous membrane appear more or less than normal with slightly vacuolated cells (triangles). (H & E, Orig. mag. X200, scale bar = 100 µm).

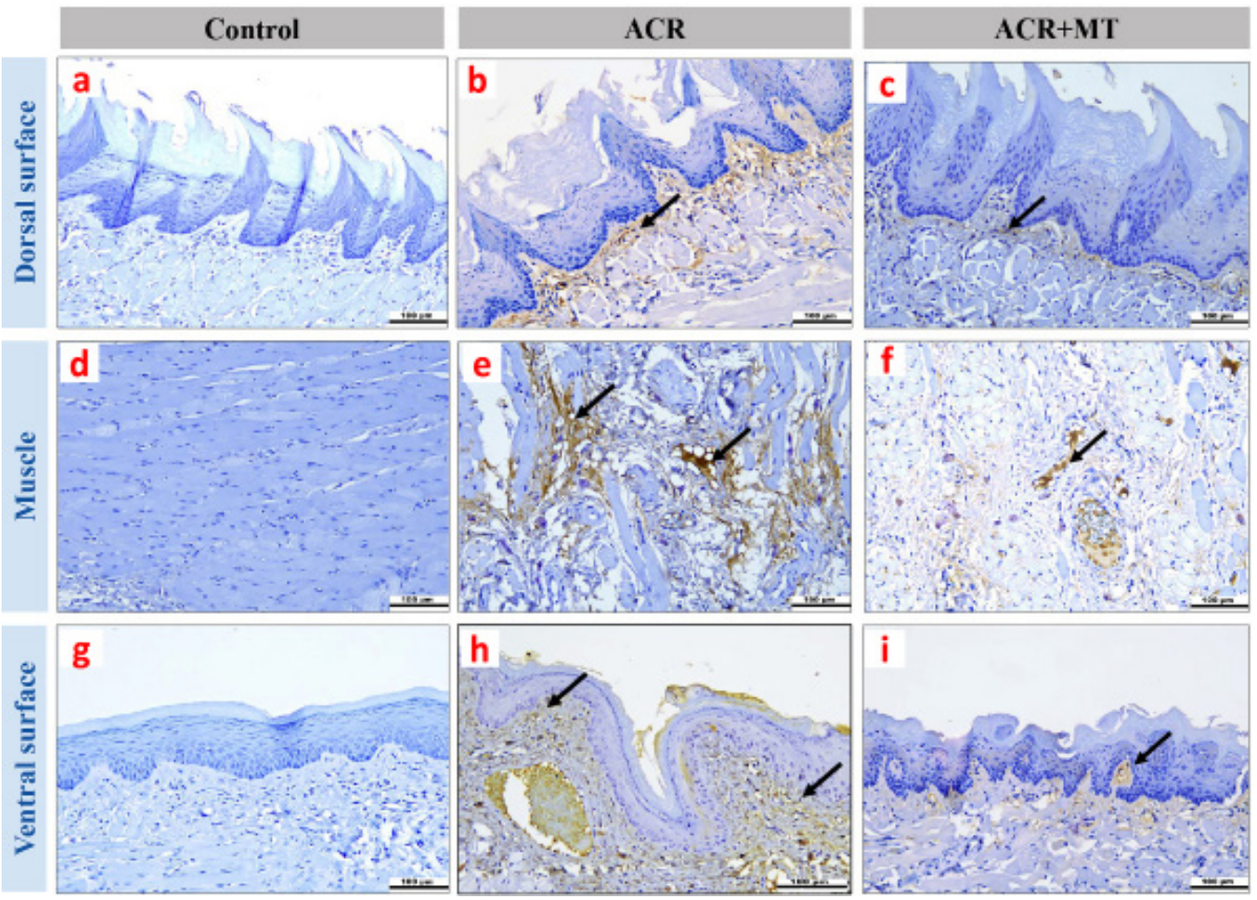

Fig. 7: A set of photomicrographs of longitudinal sections in different parts (dorsum, muscle core, ventrum) of the ant 2/3 of tongues from study groups incubated with COX-2 antibody showing:

- (a, d, g) Control group: nearly negative immunostaining.
- (b, e, h) ACR group: moderate cytoplasmic immunostaining (arrows) in the inflammatory cells of lamina propria in both dorsum and ventrum, as well as in the inflammatory cells of connective tissue of the muscle core.
- (c, f, i) ACR+ MT group: mild cytoplasmic immunostaining in the connective tissue inflammatory cells of dorsum, muscle core and ventrum (arrows).

(Anti-COX-2 antibody immunostaining: Orig. mag. X200, scale bar = 100 µm).

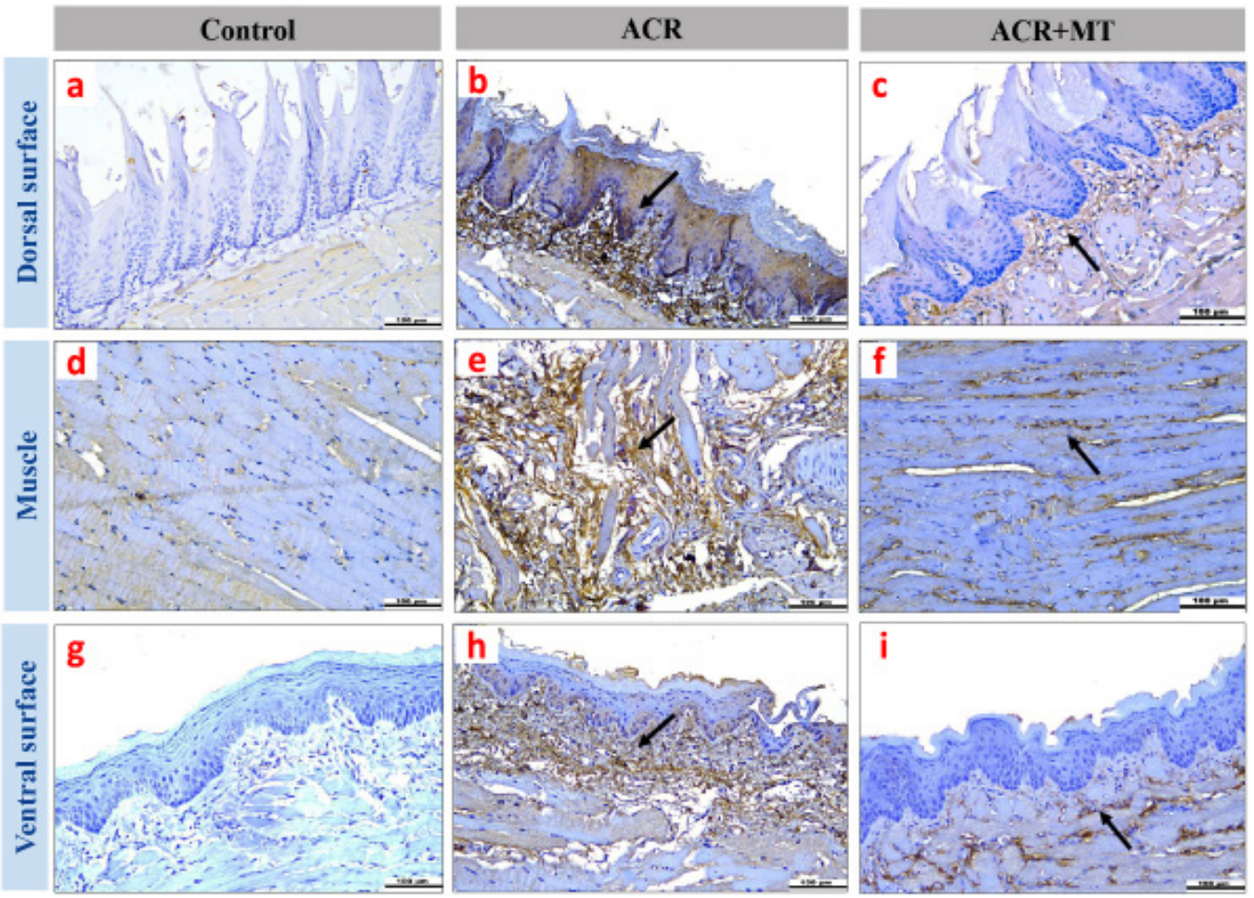

Fig. 8: A set of photomicrographs of longitudinal sections in different parts (dorsum, muscle core, ventrum) of the ant 2/3 of tongues from study groups incubated with IL1-β antibody showing:

- (a, d, g) Control group: minimal cytoplasmic immunostaining.
- (b, e, h) ACR group: intense cytoplasmic immunostaining (arrows) expressed in the epithelial cells of the dorsum, connective tissue of the muscle core, as well as, the lamina propria of both dorsum and ventrum.
- (c, f, i) ACR+ MT group: mild cytoplasmic immunostaining (arrows) in connective tissue of the muscle core, as well as, the lamina propria of both dorsum and ventrum.

(Anti-IL1-β antibody immunostaining: Orig. mag. X200, scale bar = 100 µm).

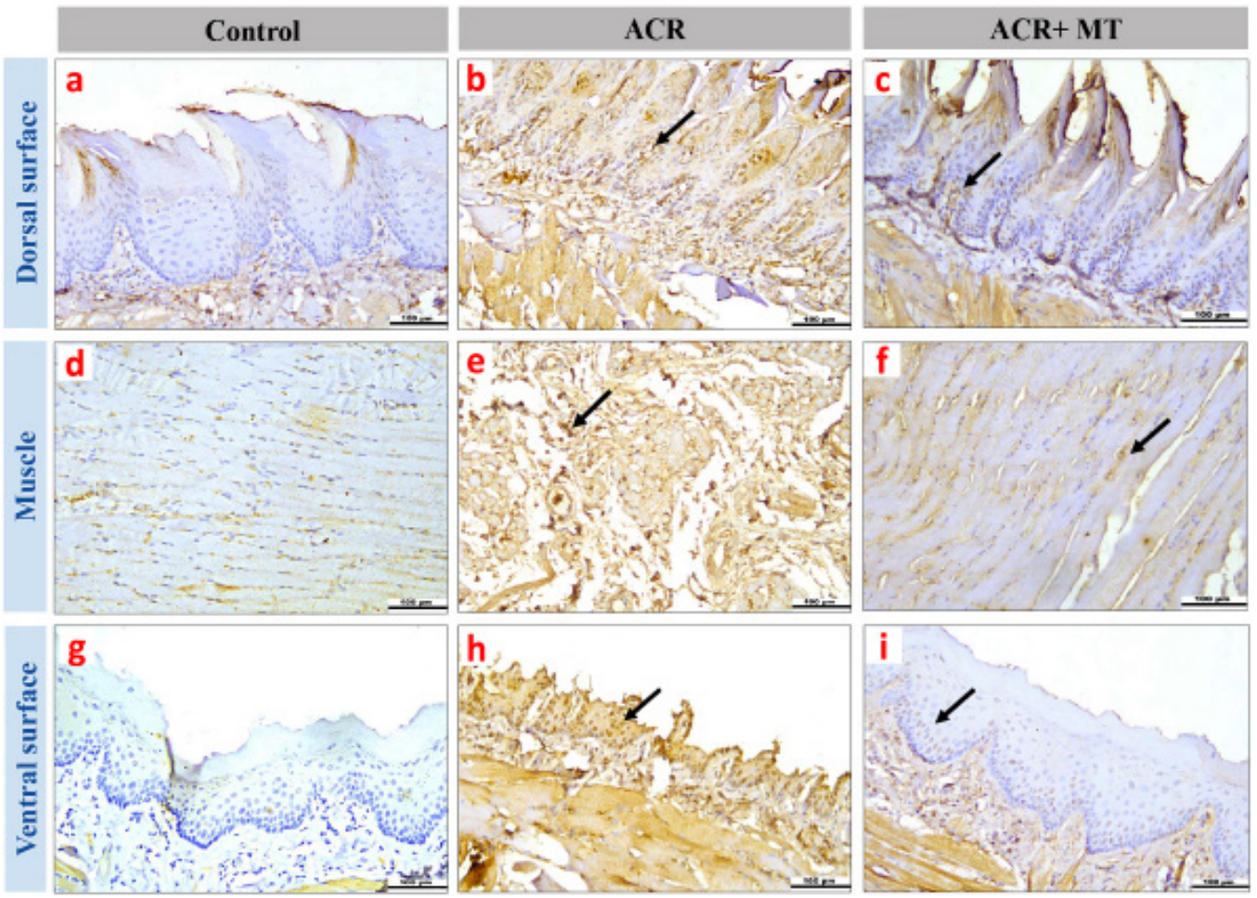

Fig. 9: A set of photomicrographs of longitudinal sections in different parts (dorsum, muscle core, ventrum) of the ant 2/3 of tongues from study groups incubated with P53 antibody showing:

- (a, d, g) Control group: minimal nuclear immunostaining of the epithelial covering of dorsum and ventrum as well as the muscle cells.
- (b, e, h) ACR group: intense nuclear immunostaining reactivity in most cells of the epithelial covering of dorsum and ventrum as well as the muscle cells (arrows).
- (c, f, i) ACR+ MT group: mild nuclear immunostaining reactivity of some cells ofthe epithelial covering of dorsum and ventrum as well as the muscle cells (arrows).

(Anti-P53 antibody immunostaining: Orig. mag. X200, scale bar = 100 µm).

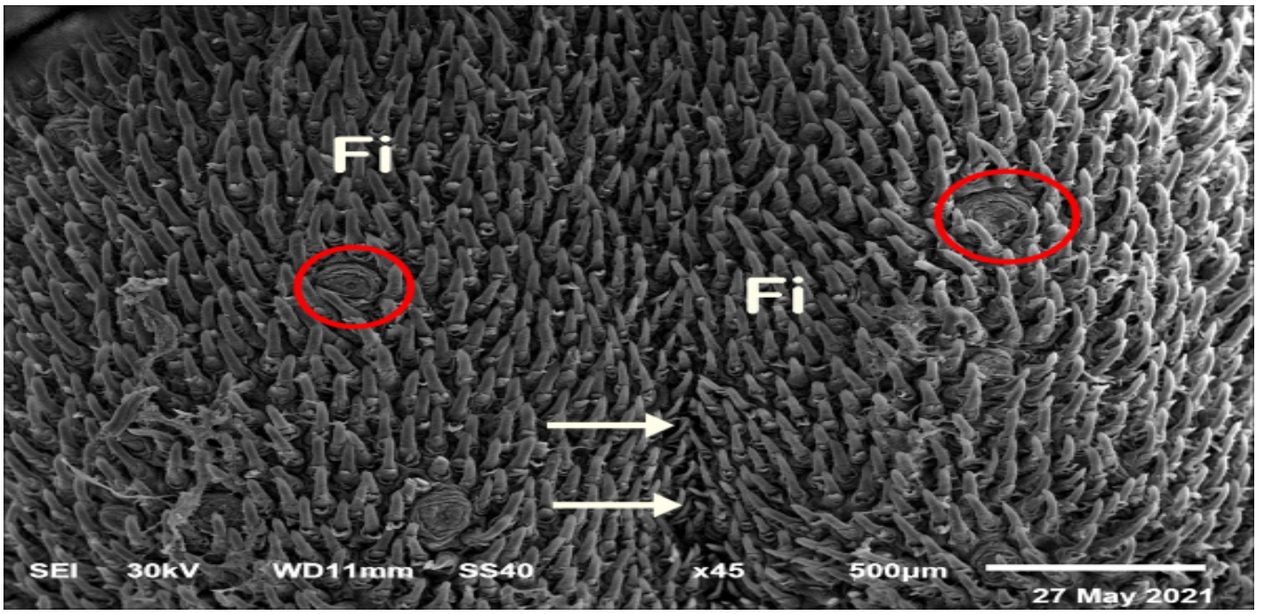

Fig. 10: A scanning electron micrograph of the dorsum of the anterior 2/3 of tongue of control group showing: Numerous conical filiform papillae with tapering ends directed caudally (Fi). Few fungiform papillae with wide apices (circles) are scattered in-between the filiform ones. Notice the median lingual sulcus (arrows). (SEM: Orig. mag. X45, scale bar = 500 µm)

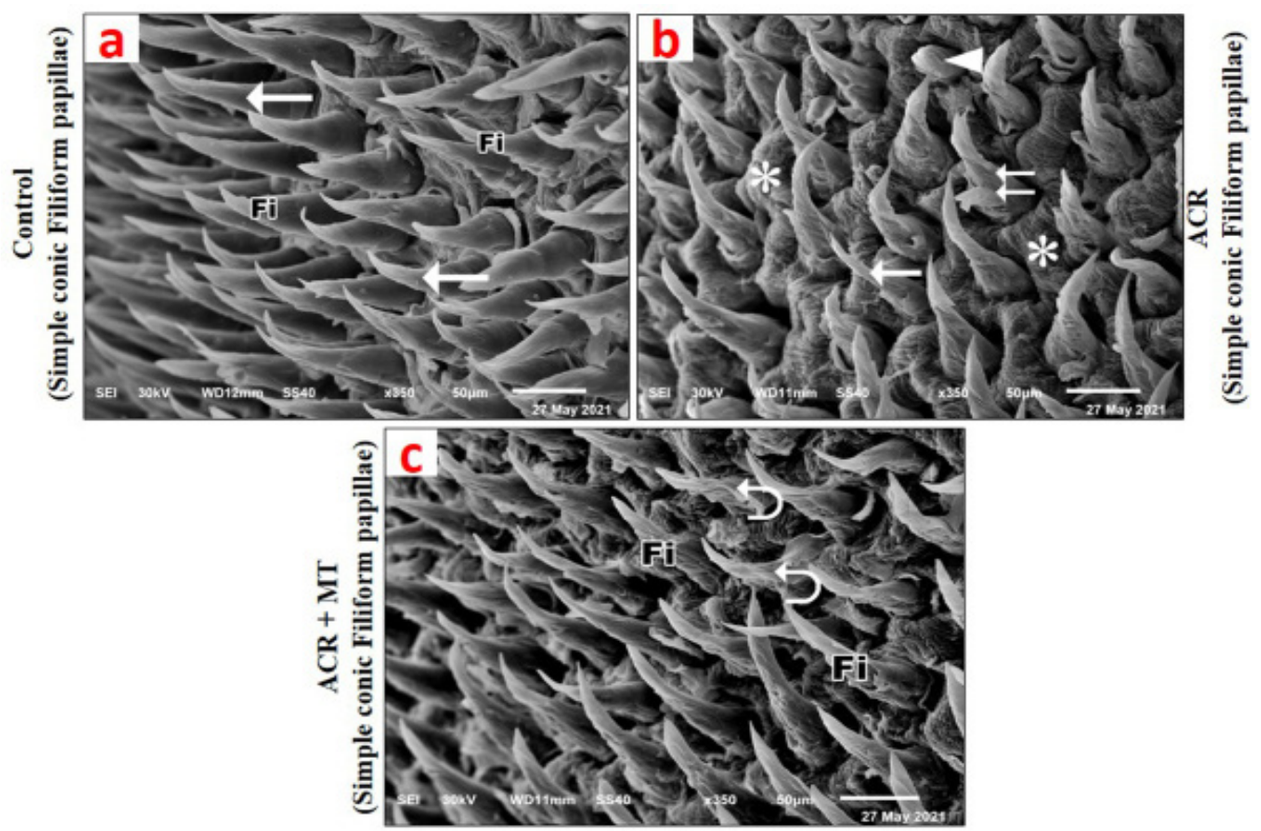

Fig. 11: A set of scanning electron micrographs of the simple conic filiform papillae of the anterior 2/3 of tongue dorsum of study groups showing: (a) control group: multiple normal filiform papillae (Fi) with elongated smooth tapering intact ends directed to the same direction (arrow). (b) ACR group: multiple degenerated widely spaced (astrikes) filiform papillae. Some papillae show broken ends (triangles), desquamation (double arrows) and thin atrophied ends (arrow). (c) ACR+ MT group: mostly nearly normal filiform papillae (Fi) with smooth tapering ends, but some papillae appear slightly thin with desquamated covering (curved arrows). (SEM: Orig. mag. X350, scale bar = 50 µm)

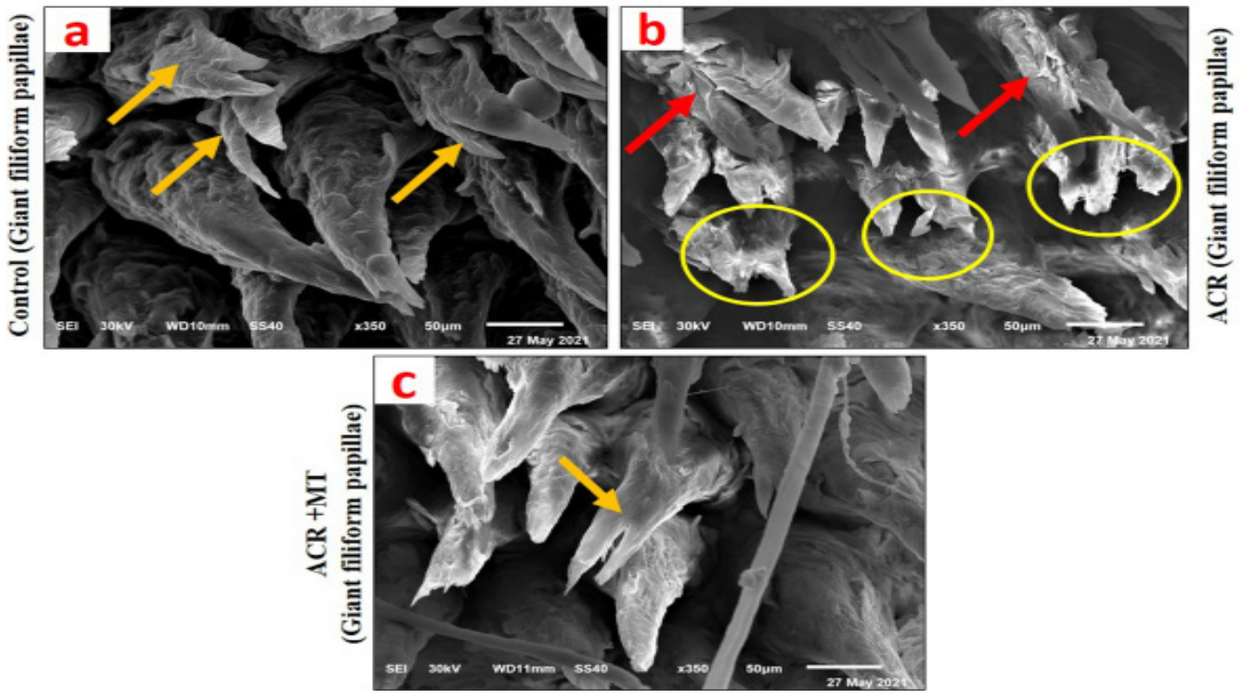

Fig. 12: A set of scanning electron micrographs of the giant filiform papillae of the anterior 2/3 of tongue dorsum of study groups showing: (a) control group: multiple normal giant filiform papillae with double tips (yellow arrows) appear healthy. (b) ACR group: multiple abnormal giant filiform papillae with broken ends (circles) and outer desquamation (red arrows). (c) ACR+ MT group: mostly nearly normal giant filiform papillae with smooth tips (yellow arrows). (SEM: Orig. mag. X350, scale bar = 50 µm)

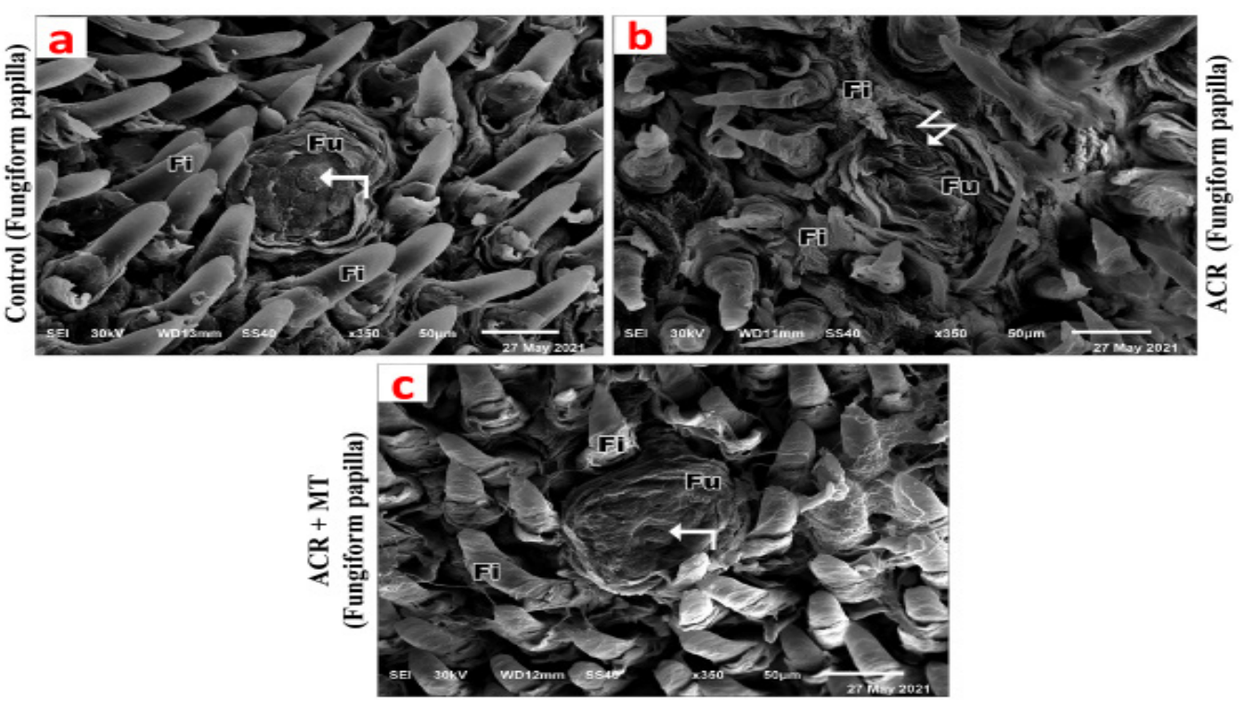

Fig. 13: A set of scanning electron micrographs of the fugiform papillae of the anterior 2/3 of tongue dorsum of study groups showing: (a) control group: broad dome shaped fungiform papillae (Fu) with flattened smooth upper surface showing taste pore (angled arrow) sporadically embedded among the filiform ones (Fi). (b) ACR group: fungiform papilla (Fu) with rough corrugated hemispherical upper portions (zigzag arrow) and ill-defined taste pore. Notice: evident atrophy of filiform papillae (Fi). (c) ACR+ MT group: mostly nearly normal fungiform papilla (Fu) with taste pore (angled arrow). (SEM: Orig. mag. X350, scale bar = 50 µm)

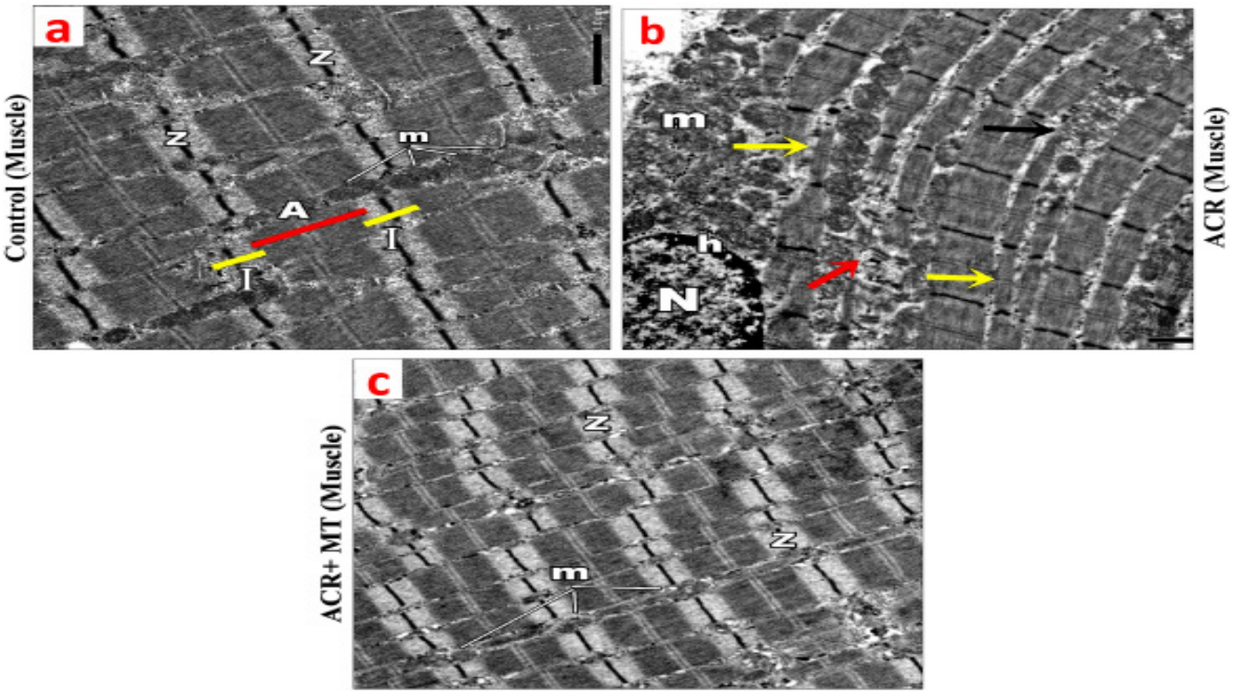

Fig. 14: A set of transmission electron micrographs of the longitudinal sections of skeletal muscle of the ant 2/3 of tongues of study groups showing: (a) Control group: The myofibrils oriented parallel to the long axis of the muscle and separated by rows of mitochondria (m). The electron-dense (Z) lines are observed. The sarcomers have alternating dark A band (red line) and light I bands (yellow lines). (b) ACR group: muscle fibers with part of the nucleus (N) displaying heterochromatin (h). Disorganized muscular striation with areas of narrowing of the myofibrils (yellow arrows). Z line irregularities are also present (red arrows). Clumps of rounded swollen mitochondria (m) with dilated cristae (black arrows) are present. (c) ACR+ MT group: nearly normal appearance of the muscle ultrastructure with restored normal striation. (SEM: Orig. mag. X5000).

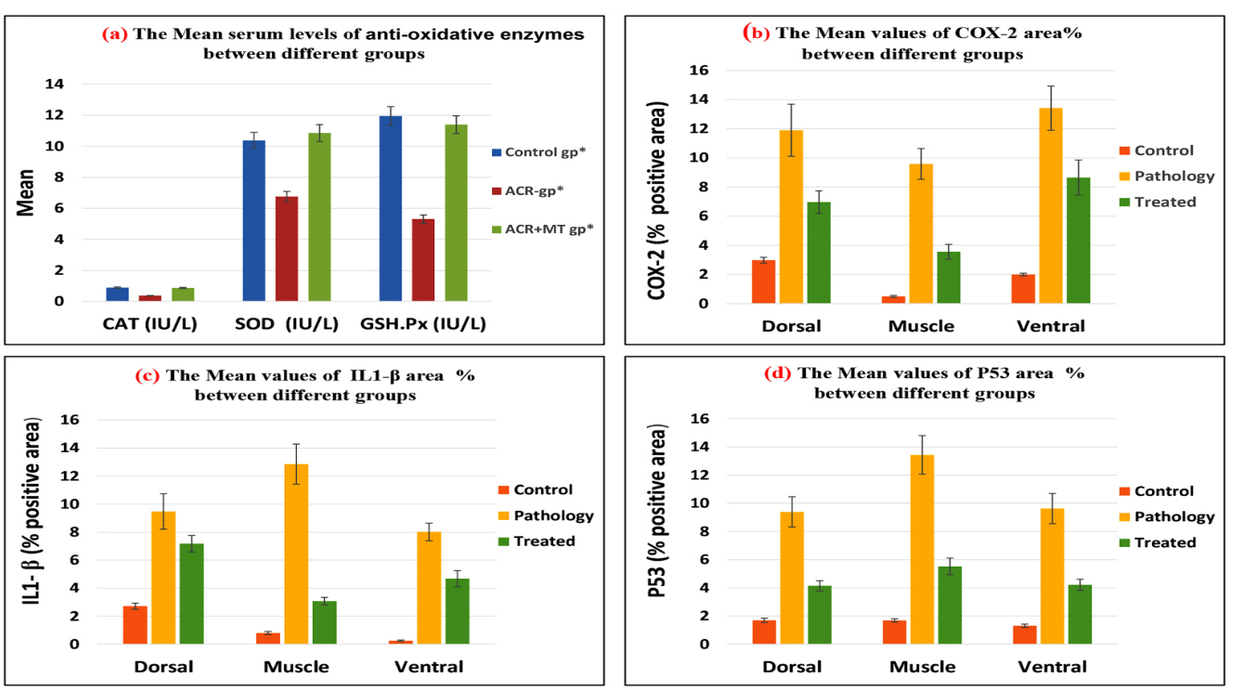

Fig. 15: representative set of histograms representing the statistical results of the study: Histogram (a): The mean values of serum levels anti-oxidatve enzymes (CAT, SOD and GSH.Px) among all the study groups. Histogram (b): The mean values of COX-2 % positive area among the study groups. Histogram (c): The mean values of IL1-β % positive area among the study groups. Histogram (d): The mean values of P53 % positive area among the study groups.

Table 1: Comparison between the mean values of different variables anti-oxidatve enzymes among three groups:

Group	Control gp*	ACR gp*	ACR+MT gp*	*P value*
CAT (IU/L)	.89±0.08	.37±0.11	.87±0.10	<0.001
SOD (IU/L)	10.38±0.89	6.76±0.93	10.86±1.39	<0.001
GSH.Px (IU/L)	11.96±1.46	5.31±0.70	11.41±1.56	<0.001

*mean ±SD

Table 2: COX-2, IL1-β and P53 area % (positively stained area fraction to total field area) in different groups:

		Control	ACR-gp	ACR+MT gp	*P value*
COX-2	Dorsal	2.98±0.20	11.90±1.79[a]	6.96±0.78[bc]	<0.001*
	Muscle	0.49±0.07	9.59±1.05[a]	3.55±0.51[bc]	
	Ventral	2.00±0.09	13.42±1.51[a]	8.66±1.20[bc]	
IL1-β	Dorsal	2.72±0.22	9.47±1.27[a]	7.18±0.59[bc]	<0.001*
	Muscle	0.81±0.10	12.85±1.43[a]	3.08±0.27[bc]	
	Ventral	0.25±0.05	8.01±0.63[a]	4.68±0.57[bc]	
P53	Dorsal	1.70±0.15	9.39±1.07[a]	4.15±0.37[bc]	<0.001*
	Muscle	1.69±0.12	13.43±1.37[a]	5.52±0.60[bc]	
	Ventral	1.31±0.12	9.63±1.08[a]	4.22±0.39[bc]	

Data expressed as Mean±SD , P:Probability *:significance <0.05
Test used: One way ANOVA followed by post-hoc tukey
a:significance between Control & Pathology groups
b: significance between Control & treated groups
c: significance between Pathology & treated groups

DISCUSSION

Recently, oral cavity and tongue disorders have increased as a result of population deterioration, new systemic diseases appearance, an adverse ecological environment, occupational conditions, and the maintenance of bad behaviors which impact oral health negatively[24]. The rat tongue has papillae, like the human tongue dorsum. But in rats, filiform papillae involves; simple conic papillae (present on the anterior two thirds of the tongue dorsum), true papillae (present on the intermolar prominence), and giant papillae with 2 tips (present between the previous two types). Between the filiform papillae, there are small number of fungiform papillae (mushroom-like) that contains the taste buds in the epithelium of the upper part[25].

Growing evidences revealed that Acrylamide has carcinogenic effect to humans[26]. Previous researches focused on lowering ACR levels in foods by altering processing settings. However, the presence of ACR in food is inevitable. Because of its high water solubility and little molecular weight, it may simply passes the body membranes, be absorbed in the GIT, and dispersed all over the body[27]. Nevertheless, there is limited published work on ACR influence on lingual histology, as well as scant information on preventive methods. As a consequence, the primary target of our study was to determine (i) if ACR over a short length of time may cause changes in the lingual structure, and (ii) whether Mito-TEMPO can protect against ACR-induced lingual toxicity. We investigated these issues in a rat model of ACR toxicity utilizing biochemical, histological, immunohistochemical and electron microscopy approaches.

According to our findings in Group II, the antioxidant system in rats collapsed as a result of severe oxidative stress brought on by ACR that was more than the load it could handle, as evidenced by a significant decline (p<0.001) in the antioxidant enzymatic activity measurements (CAT, SOD and GSH.Px). These findings are consistent with prior researches[28,29]. Furthermore, the L/M outcomes of this study clearly indicated that ACR treatment generated obvious structural alterations in the tongue mucosa on the dorsal and ventral surfaces, as well as the muscle core. These abnormalities included lingual papillae distortion (both filiform and fungiform), atrophied mucosa with thin keratin coating, fragmented muscle fibers, congested blood vessels in the muscle core. Other essential finding reported in ACR group in this study was the presence foci of sebaceous gland-like metaplasia in the dorsal mucous membrane.

The E/M results supported the previous findings. The electron micrographs revealed atrophied papillae (simple conic filiform papillae, giant filiform papillae and fungiform papillae), disorganized myofibrils and distorted mitochondria of the muscular core compared to the control group.

In addition, ACR statistically significant raised (p<0.001) the lingual immunoreactivity for COX-2 (oxidative marker), IL1-β (pro-inflammatory marker) and P53 (apoptotic marker) as related to the control group.

Our findings agreed with previously reported data. Previous researchers[30] declared that neonates of mothers who were fed with potato chips or consumed ACR therapy showed atrophy of lingual filiform and fungiform papillae with essentially no apical keratin layers. Also,[31] showed that ACR had the same toxicological impact on the lingual skeletal muscle. A previous study also showed rat oral epithelium underwent similar sebaceous metaplasia after chemical carcinogenesis with 4-nitrotiuinoline N-oxide[32]. This might be attributed to GA, which, being a genotoxic carcinogen, binds covalently to DNA, causes mutations, cellular changes leading to cancer. This can explain the sebaceous gland metaplasia in the dorsal papillae ACR intoxicated rats[33].

To clarify the mechanisms by which ACR induces toxicity,[34] showed that when taken orally, ACR reaches the bloodstream and circulates to many tissues where it interacts with nucleic acids, nerve cells, RBCs hemoglobin, and important enzymes to cause a variety of negative effects. Acrylamide thus enhances cell damage by different mechanisms, as oxidative stress, inflammatory responses, apoptosis, and DNA damage.

The body has a number of protective mechanisms to combat the harmful effects of free radicals[6]. A complicated array of antioxidant defense systems, including catalase, superoxide dismutase, and glutathione peroxidase/ reductase, keep intracellular ROS levels in control[35]. SOD immediately transforms superoxide anion to hydrogen peroxide, and the two key enzymes, GSH.Px and CAT, are then participate in the detoxification of H2O2 in a cellular antioxidant defense way[36].

ACR has tight link to oxidative stress in recent researches. It disrupts the cell redox pathway by producing reactive oxygen radicals. Moreover, ACR is converted to the active metabolite glycidamide (GA) which subsequently combined with glutathione (GSH)[37]. Compared to the original acrylamide chemical, glycidamide is more reactive towards aminoacids, lipids, and nucleic acids[38].

The reservoir of cellular antioxidant enzymes is reduced when ACR concentration rises[39]. As a result, previous research has shown that oxidative stress-induced apoptosis is caused by ACR metabolism due to increased oxidative stress-related fat peroxidation and mitochondrial malfunction[40]. Later, this mitochondrial dysfunction causes increased expression of COX-2, a pro-inflammatory mediator[41]. COX-2 is a critical enzyme that serves as the primary source of prostaglandins (PG), it is universally viewed as a pathology-related enzyme that is mostly responsible for inflammation[42]. As a cascade, overexpression of COX-2 exerts apoptotic effects through the initiation of p53, suggesting functional interactions of COX-2 with p53[43].

Several inflammatory mediators, including TNF-, IL-1, and IL-6, were found to be increased during damage caused by acrylamide[44]. These pro-inflammatory mediators in turn cause overexpression of COX-2[45], and the increased expression of IL1-β further promotes ACR's pro-inflammatory impact[46].

On the other hand, mitochondria are the first organoids to be harmed by ROS because of their close proximity to ROS production[47]. As a result, ROS has arisen as an eye-catching therapeutic goal, with numerous drug-based approaches aiming to enhance cellular antioxidant capability and boost ROS cleaning[48]. Several innovative antioxidants which particularly target mitochondria, have been proven for the treatment of oxidative stress-associated disorders[49].

Mito-TEMPO, a selective mitochondrial antioxidant, is composed of two chemical components; the antioxidant TEMPO, linked to the lipophilic molecule triphenylphosphonium (TPP)[50]. TEMPO is known as superoxide dismutase (SOD) derivative[51]. It is delivered to mitochondria and works as ROS trap[52]. On the other hand, the positively charged lipophilic TPP serves as the mitochondria-targeting molecule, allowing Mito-TEMPO to bypass the lipid bilayer into the mitochondrial fluid, where it becomes 1000-fold greater concentrations than in other sites[53]. Conflicting publications have been reported to demonstrate the wide protective benefits of Mito-TEMPO in various pathological models[54,55,56]. However, to the best of our knowledge, this is the first time a mitochondrial-targeted antioxidant has been used to prevent ACR-induced lingual toxicity.

In this context, our outcomes established the antioxidant, anti-inflammatory and anti-apoptotic effects of Mito-TEMPO on ACR lingual toxicity, suggesting the use of Mito-TEMPO to prevent or delay harmful effects caused by ACR exposure. Mito-TEMPO showed statistically significant rise (P<0.001) in the antioxidant defense enzymes CAT, SOD and GSH.Px, suggesting that Mito-TEMPO can normalize the oxidative stress. Our next step was to demonstrate histologically the effect of Mito-TEMPO pretreatment on ACR lingual toxicity in group III.

This group showed improvement in all histological results. The dorsal surfaces with their lingual papillae, the muscle core and the ventral surfaces showed apparent improvement of the histological architectures by light microscope, TEM and SEM. The different parts of the tongue appeared nearly normal. Regarding the immunohistochemical results, this group showed statistically significant decline (P< 0.001) in COX-2, IL1-β and P53 area percent. These outcomes are consistent with earlier researches used Mito-TEMPO pretreatment that alleviated inflammation, mitigated LPS-induced liver injury, and improved the anti-oxidative capability in toxic mice model[57], and renal sepsis model[58].

In line with our findings, previous research also has revealed that Mito-TEMPO has a greater therapeutic time window for protecting against acetaminophen-induced hepatotoxicity[59,60] In addition, systemic treatment of Mito-TEMPO was able to ameliorate ischemic brain injury in rats[61]. Mito-TEMPO also protected against podocyte injury by inhibiting inflammatory pathways[62].

Taken together, these results show that Mito-TEMPO may keep the mitochondrial integrity that could enhance cell survival by hindering the formation of ROS-associated cell death[63].

CONCLUSION

Acrylamide is toxic to the rat tongue mucosa and underlying muscle, which results in considerable serological, histological, immunohistochemical, and ultrastructural changes. Therefore, we think Mito-TEMPO has excellent protective potential and should be included in preventive and therapeutic approaches to ACR toxicity. Further researches are required to clarify the time dependence and, in particular, the long-term effects of using Mito-TEMPO after chronic ACR exposure. Also, we need to demonstrate the therapeutic effect of Mito- TEMPO in different animal models of ACR-induced toxicity.

CONFLICT OF INTERESTS

There are no conflicts of interest.

REFERENCES

1. Erriu M, Pili FM, Cadoni S, Garau V. (2016): Diagnosis of Lingual Atrophic Conditions: Associations with Local and Systemic Factors. A Descriptive Review. Open Dent J. 16; 10: 619-635.
2. Hutanu E, Damian A, Micl ˘aus V, Rat,iu IA, Rus V, Vlasiuc I, Gal AF. (2022): Morphometric Features and Microanatomy of the Lingual Filiform Papillae in the Wistar Rat. Biology (Basel).;11(6) :920.
3. Wei Q, Li J, Li X, Zhang L, Shi F. (2014): Reproductive toxicity in acrylamide-treated female mice. Reprod. Toxicol.; 46: 121–128.
4. Virk-Baker MK, Nagy TR, Barnes S, Groopman J. (2014): Dietary acrylamide and human cancer: a systematic review of literature. Nutr Cancer.; 66(5): 774-790.
5. Basaran B, Faiz O. (2022): Determining the Levels of Acrylamide in Some Traditional Foods Unique to Turkey and Risk Assessment. Iran J Pharm Res.; 21(1):e123948.
6. Ahmed G, Fahad A, Misfer A, Mohamed A, Ammar AL F, Mohamed A. (2020): A Review on the New Trends of Acrylamide Toxicity. Biomed J Sci & Tech Res 27(2). BJSTR. MS.ID.004480.
7. Mojska H, Gielecińska I, Stoś K. (2012): Determination of acrylamide level in commercial baby foods and an assessment of infant dietary exposure. Food Chem Toxicol.; 50(8):2722-8.
8. Park JS, Samanta P, Lee S, Lee J, Cho JW, Chun HS, Yoon S, Kim WK. (2021): Developmental and Neurotoxicity of Acrylamide to Zebrafish. Int J Mol Sci.; 22(7):3518.
9. Başaran B, Çuvalcı B, Kaban G. (2023): Dietary Acrylamide Exposure and Cancer Risk: A Systematic Approach to Human Epidemiological Studies. Foods.; 12(2):346.
10. Yildizbayrak N and Erkan M. (2018). Acrylamide disrupts the steroidogenic pathway in Leydig cells: Possible mechanism of action. Toxicological and Environmental Chemistry.; 100(2): 235–246.
11. Yang Y, Zhang L, Jiang G, Lei A, Yu Q, Xie J, Chen Y. (2019): Evaluation of the protective effects of Ganoderma atrum polysaccharide on acrylamide-induced injury in small intestine tissue of rats. Food Funct.; 10(9):5863-5872.
12. Crozier A, Jaganath IB, Clifford MN. (2009): Dietary phenolics: Chemistry, bioavailability and effects on health. Nat Prod Rep; 26(8): 1001–1043.
13. Poljsak B, Šuput D, Milisav I. (2013): Achieving the Balance between ROS and Antioxidants: When to Use the Synthetic Antioxidants. Oxid. Med. Cell. Longev. 2013, 956792.
14. Abdullah-Al-Shoeb M, Sasaki K, Kikutani S, Namba N, Ueno K, Kondo Y, Maeda H, Maruyama T, Irie T, Ishitsuka Y. (2020): The Late-Stage Protective Effect of Mito-TEMPO against Acetaminophen-Induced Hepatotoxicity in Mouse and Three-Dimensional Cell Culture Models. Antioxidants (Basel).; 9(10):965.
15. Ghorbel I, Elwej A, Chaabene M, Boudawara O, Marrakchi R, Jamoussi K, Boudawara TS, Zeghal N. (2017): Effects of acrylamide graded doses on metallothioneins I and II induction and DNA fragmentation: Bochemical and histomorphological changes in the liver of adult rats. Toxicol Ind Health.; 33(8):611-622.
16. Zhan L, Li R, Sun Y, Dou M, Yang W, He S, Zhang Y. (2018): Effect of mito-TEMPO, a mitochondria-targeted antioxidant, in rats with neuropathic pain. Neuroreport.; 29(15):1275-1281.
17. Aebi H. (1984): Catalase in *vitro*. Methods Enzymol. 105, 121–126.
18. Fridovich I. (1989): Superoxide dismutase: An adaptation to a paramagnetic gas. J. Biol Chem. 264, 7761– 7764.
19. Paglia DE, Valentine WN. (1967): Studies on the quantitative and qualitative characterization of erythrocyte glutathione peroxidase. J. Lab. Clin Med. 70, 158–169. 19.
20. Sanderson T, Wild G, Cull AM, Marston J, Zardin G. Suvarna SK, Layton C, Bancroft JD. (2019): Immunohistochemical and immunofluorescent techniques. Bancroft's Theory and Practice of Histological Techniques. 8th ed. p.337–394. Elsevier; London.

21. Renshaw, S. (2017): Immunohistochemistry and immunocytochemistry. 2nd ed. Chapter 3 immunohistochemistry and cytochemistry. Pp 35-101. Wiley Blackwell.

22. Woods AE, Stirling JW. (2018): Transmission electron microscopy. In: Bancroft's theory and practice of histological techniques, pp 434–475

23. Ibrahim MAAH, Elwan WM. (2019): Effect of irinotecan on the tongue mucosa of juvenile male albino rat at adulthood. Int J Exp Pathol.; 100(4):244-252.

24. Davydova L, Tkach G, Tymoshenko A, Moskalenko A, Sikora V, Kyptenko L, Lyndin M, Muravskyi D, Maksymova O, Suchonos O. (2017): Anatomical and morphological aspects of papillae, epithelium, muscles, and glands of rats' tongue: Light, scanning, and transmission electron microscopic study. Interv Med Appl Sci.; 9(3):168-177.

25. Costa AC, Pereira CA, Junqueira JC, Jorge AO. (2013): Recent mouse and rat methods for the study of experimental oral candidiasis. Virulence; 4(5):391-9.

26. Mucci LA, Dickman P, Steineck G, Adami H-O, Augustsson K. (2003): Dietary acrylamide and cancer of the large bowel, kidney, and bladder: absence of an association in a population-based study in Sweden. British Journal of Cancer; 88(1); 84–89.

27. Zhao S, Zhao X, Liu Q, Jiang Y, Li Y, Feng W, Xu H, Shao M. (2020): Protective effect of Lactobacillus plantarum ATCC8014 on acrylamide-induced oxidative damage in rats. Appl Biol Chem: 63 (1); 43.

28. Guo J, Cao X, Hu X, Li S, Wang J. (2020): The anti-apoptotic, antioxidant and anti-inflammatory effects of curcumin on acrylamide-induced neurotoxicity in rats. BMC Pharmacology and Toxicology.;21(1):1-10

29. Gur C, Kandemir FM, Darendelioglu E, Caglayan C, Kucukler S, Kandemir O, Ileriturk M. (2021): Morin protects against acrylamide-induced neurotoxicity in rats: an investigation into different signal pathways. Environ Sci Pollut Res Int.; 28(36):49808-49819.

30. El-Sayyad HIH, Khalifa SA, Fahmy AAE, El-Shahary EA, Ibrahim EMA (2017): Abnormal Soft Palate, Lingual Mucosa and Intestine of Neonates Maternally Fed on Diet Containing Fried Potatoes Chips or Received Acrylamide-Treatment. J Pharma Reports 2: 134.

31. Al-Serwi RH, Ghoneim FM. (2015): The impact of vitamin E against acrylamide induced toxicity on skeletal muscles of adult male albino rat tongue: Light and electron microscopic study. J Microsc Ultrastruct.; 3(3):137-147.

32. FISKER AV, PHILIPSEN HP. (1983): Sebaceous metaplasia of rat oral epithelium during chemical carciuogenesis. J Cutanous Path; 10: 164-170.

33. Mei N, McDaniel LP, Dobrovolsky VN, Guo X, Shaddock JG, Mittelstaedt RA, Azuma M, Shelton SD, McGarrity LJ, Doerge DR, Heflich RH. The genotoxicity of acrylamide and glycidamide in big blue rats. Toxicol Sci.; 115(2):412-421.

34. Rayburn JR, Friedman M. (2010): L-cysteine, N-acetyl-L-cysteine, and glutathione protect Xenopus laevis embryos against acrylamide-induced malformations and mortality in the frog embryo teratogenesis assay. J Agric Food Chem.; 58(20):11172-8.

35. Kim SA, Jang JH, Kim W, Lee PR, Kim YH, Vang H, Lee K, Oh SB. (2022): Mitochondrial Reactive Oxygen Species Elicit Acute and Chronic Itch via Transient Receptor Potential Canonical 3 Activation in Mice. Neurosci Bull.; 38(4):373-385.

36. Song MH, Kim HN, Lim Y, Jang IS. (2017); Effects of coenzyme Q10 on the antioxidant system in SD rats exposed to lipopolysaccharide-induced toxicity. Lab Anim Res.; 33(1):24-31.

37. Hu C, Zhang H, Qiao Z, Wang Y, Zhang P, Yang D. (2018): Loss of thioredoxin 2 alters mitochondrial respiratory function and induces cardiomyocyte hypertrophy. Exp Cell Res.; 372(1):61-72.

38. Salimi A, Baghal E, Ghobadi H, Hashemidanesh N, Khodaparast F, Seydi E. Mitochondrial, lysosomal and DNA damages induced by acrylamide attenuate by ellagic acid in human lymphocyte. PLoS One.; 16(2):e0247776.

39. Kunnel SG, Subramanya S, Satapathy P, Sahoo I, Zameer F.(2019): Acrylamide Induced Toxicity and the Propensity of Phytochemicals in Amelioration: A Review. Cent Nerv Syst Agents Med Chem.; 19(2):100-113.

40. Yuan Y, Yucai L, Lu L, Hui L, Yong P, Yan Haiyang Y. (2022). Acrylamide induces ferroptosis in HSC-T6 cells by causing antioxidant imbalance of the XCT-GSH-GPX4 signaling and mitochondrial dysfunction. Toxicology Letters.; 368(1): 24-32.

41. Chen, C. (2010): COX-2's new role in inflammation. Nat Chem Biol 6, 401–402

42. Ju Z, Lia M, Xua J, Howella DC, Zhiyun Lia Z, Chena F-E. (2022): Recent development on COX-2 inhibitors as promising anti-inflammatory agents: The past 10 years. Acta Pharmaceutica Sinica B.; 12(6): 2790-2807

43. Han JA, Kim JI, Ongusaha PP, Hwang DH, Ballou LR, Mahale A, Aaronson SA, Lee SW. (2002): P53-mediated induction of Cox-2 counteracts p53- or genotoxic stress-induced apoptosis. EMBO J.; 21(21):5635-44.

44. Pan X, Wu X, Yan D, Peng C, Rao C, Yan H. (2018): Acrylamide-induced oxidative stress and inflammatory response are alleviated by N-acetylcysteine in PC12 cells: Involvement of the crosstalk between Nrf2 and NF-κB pathways regulated by MAPKs. Toxicol Lett; 288:55-64.

45. Yang CM, Yang CC, Hsiao LD, Yu CY, Tseng HC, Hsu CK, Situmorang JH. (2021): Upregulation of COX-2 and PGE2 Induced by TNF-α Mediated Through TNFR1/MitoROS/PKCα/P38 MAPK, JNK1/2/FoxO1 Cascade in Human Cardiac Fibroblasts. J Inflamm Res.; 14: 2807-2824.

46. Liu Z, Song G, Zou C, Liu G, Wu W, Yuan T, Liu X. (2015): Acrylamide induces mitochondrial dysfunction and apoptosis in BV-2 microglial cells. Free Radic Biol Med.; 84:42-53.

47. Chen JW, Ma PW, Yuan H, Wang WL, Lu PH, Ding XR, Lun YQ, Yang Q, Lu LJ.(2022): mito-TEMPO Attenuates Oxidative Stress and Mitochondrial Dysfunction in Noise-Induced Hearing Loss via Maintaining TFAM-mtDNA Interaction and Mitochondrial Biogenesis. Front Cell Neurosci. 8; 16: 803718.

48. Peoples JN, Saraf A, Ghazal N, Pham TT, Kwong JQ. (2019): Mitochondrial dysfunction and oxidative stress in heart disease. Exp Mol Med.; 51(12):1-13.

49. Zinovkin RA, Zamyatnin AA. (2019): Mitochondria-Targeted Drugs. Curr Mol Pharmacol.; 12(3):202-214.

50. Trnka J, Blaikie FH, Smith RA, Murphy MP. (2007): A mitochondria-targeted nitroxide is reduced to its hydroxylamine by ubiquinol in mitochondria. Free Radic Biol Med.; 44(7):1406-1419.

51. Johri, A. (2021): Disentangling Mitochondria in Alzheimer'sDisease. Int. J. Mol. Sci., 22, 11520.

52. Weidinger A, Birgisdóttir L, Schäffer J, Meszaros AT, Zavadskis S, Müllebner A, Hecker M, Duvigneau JC, Sommer N, Kozlov AV. (2022): Systemic Effects of mitoTEMPO upon Lipopolysaccharide Challenge Are Due to Its Antioxidant Part, While Local Effects in the Lung Are Due to Triphenylphosphonium. Antioxidants (Basel).; 11(2):323.

53. Fujii Y, Matsumura H, Yamazaki S, Shirasu A, Nakakura H, Ogihara T, Ashida A (2020): Efficacy of a mitochondrion-targeting agent for reducing the level of urinary protein in rats with puromycin aminonucleoside-induced minimalchange nephrotic syndrome. PLoS ONE 15(1): e0227414.

54. Wu J, Zheng L, Mo J, Yao X, Fan C, Bao Y. (2020): Protective Effects of MitoTEMPO on Nonalcoholic Fatty Liver Disease via Regulating Myeloid-Derived Suppressor Cells and Inflammation in Mice. Biomed Res Int.: 9329427; 1-9.

55. Tuncer S, Akkoca A, Celen MC, Dalkilic N. (2021): Can MitoTEMPO protect rat sciatic nerve against ischemia-reperfusion injury? Naunyn-schmiedeberg's Archives of Pharmacology.; 394(3):545-553.

56. Yildiz E, Ayvat P, Sahin AS, Piskin MM, Soner BC. (2022): Protective effect of mitotempo in streptozotocin-induced diabetic rat model: Effects on corpus cavernosum and aorta. Journal of Advanced Research in Health Sciences; 5(2):82-87.

57. Wang PF, Xie K, Cao YX, Zhang A. (2022): Hepatoprotective Effect of Mitochondria-Targeted Antioxidant Mito-TEMPO against Lipopolysaccharide-Induced Liver Injury in Mouse. Mediators Inflamm; Article ID: 6394199.

58. Arulkumaran N, Pollen SJ, Tidswell R, Gaupp C, Peters VBM, Stanzani G, Snow TAC, Duchen MR, Singer M. (2021): Selective mitochondrial antioxidant MitoTEMPO reduces renal dysfunction and systemic inflammation in experimental sepsis in rats. Br. J. Anaesth.; 127:577–586.

59. Du K, Farhood A, Jaeschke H. (2017): Mitochondria-targeted antioxidant Mito-Tempo protects against acetaminophen hepatotoxicity. Arch Toxicol.; 91(2):761-773.

60. Abdullah-Al-Shoeb M, Sasaki K, Kikutani S, Namba N, Ueno K, Kondo Y, Maeda H, Maruyama T, Irie T, Ishitsuka Y. (2020): The Late-Stage Protective Effect of Mito-TEMPO against Acetaminophen-Induced Hepatotoxicity in Mouse and Three-Dimensional Cell Culture Models. Antioxidants (Basel); 9(10):965.

61. Li C, Sun H, Xu G, McCarter KD, Li J, Mayhan WG. (2018): Mito-Tempo prevents nicotine-induced exacerbation of ischemic brain damage. J Appl Physiol; 125(1): 49-57.

62. Liu B, Wang D, Cao Y, Wu J, Zhou Y, Wu W, Wu J, Zhou J, Qiu J. (2022): MitoTEMPO protects against podocyte injury by inhibiting NLRP3 inflammasome via PINK1/Parkin pathway-mediated mitophagy. Eur J Pharmacol. 15; 929: 175136.

63. Mukem S, Thongbuakaew T, Khornchatri K. (2021): Mito-Tempo suppresses autophagic flux via the PI3K/Akt/mTOR signaling pathway in neuroblastoma SH-SY5Y cells. Heliyon; 7:e07310. 1-9.

الملخص العربى

الميتوتمبو: أحد مضادات الأكسدة الانتقائية للميتوكندريا، يخفف من الضرر الناتج عن ماده الأكرالاميد في الثلثين الأماميين من اللسان في الجرذان. دراسة كيميائية وهستولوجية وهستوكيميائية مناعيه

هبة بيومي[١]، ايناس الجندي[١]، هاله طه شعلان[٢]، ابتسام بدير[٣]، نشوى السيد[٤]، اميرة الألفي[١]

[١]قسم الأنسجة و بيولوجيا الخلية، [٤]قسم الكيمياء الطبية والبيولوجيا الجزيئية، كلية الطب البشري، جامعة بنها، مصر

[٢]قسم التشريح و الاجنة ـ كلية الطب ـجامعه عين شمس ـ مصر

[٣]قسم الطب الشرعي و السموم الاكلينيكية ـ كلية الطب البيطري ـ جامعة بنها- مصر

المقدمة: مادة الأكريلاميد هي مادة سامة شائعة. ويعد تعرض الانسان و الحيوان للأكرالاميد خلال النظام الغذائي أحد أهم القضايا الصحية في جميع أنحاء العالم في الوقت الحالي. و قد حظيت مضادات الأكسدة الغذائية بالاهتمام كاستراتيجية وقائية محتملة وكمكمل غذائي لمعالجة مختلف السموم التي يسببها الأكرالاميد.

هدف البحث: دراسة التأثير الوقائي المحتمل لعقار الميتوتمبوعلى سمية اللسان الناجمة عن مادة الأكريلاميد.

المواد و الطرق المستخدمة: تم تقسيم اثنين وثلاثين من ذكور الجرذ البالغة إلى ٣ مجموعات. المجموعة الأولى (المجموعة الضابطة). المجموعة الثانية (مجموعة الأكرالاميد): عولجت الجرذان بـ ٤٠ ملجم / كجم / يوميا من ماده الأكريلاميد مذاب في محلول ملحي عن طريق الفم بالتزقيم لمدة ١٤ يومًا. المجموعة الثالثة (مجموعة المايتوتمبو+ الأكرالاميد): عولجت الفئران مثل المجموعه الثانيه بالاكرالاميد. حُقنت بـ ٠,٧ مجم / كجم من المايتوتمبو داخل الصفاق مرة واحدة يوميًا لمدة يومين قبل مادة الأكريلاميد واستمرحقنها مع مادة الأكريلاميد لمدة ١٤ يومًا أخرى. (يعطى الميتوتمبو قبل ماده الأكرالاميد ب ٣٠).

النتائج: أظهرت المجموعة المعالجة بالأكريلاميد انخفاضًا ملحوظا (P <٠,٠٠١) في مستويات الإنزيمات المضاده للاكسده، واظهر الفحص بالمجهر الضوئي والالكتروني تغيرات مرضية ملحوظة في كلا السطحين والعضلات الأساسية والذي شمل تدهور حليمات اللسان وتشوه العضلات وضمورالأغشية المخاطية. كانت هناك زيادة ملحوظه (P<٠,٠٠١) في التفاعل المناعي لـبروتين سيكلواوكسيجيناز ٢ و انترلوكين ١- بيتا و بي ٥٣ في جميع مناطق اللسان التي تم فحصها. أظهرت المجموعة المعالجة مسبقًا بعقار الميتوتمبو زيادة (P <٠,٠٠١) في الإنزيمات المضاده للاكسده مع تحسن واضح في التركيب النسيجي وانخفاض التفاعل المناعي (P <٠,٠٠١) لبروتين سيكلواوكسيجيناز ٢ وانترلوكين ١- بيتا و بي ٥٣.

الإستنتاج: كشفت الدراسه عن تأثير وقائي محتمل لعقار الميتوتمبو على سمية اللسان الناجمة عن مادة الأكريلاميد.